

Article

Use of Foundry Sands in the Production of Ceramic and Geopolymers for Sustainable Construction Materials

Caterina Sgarlata ^{1,2}, Maria Camila Ariza-Tarazona ¹, Enrico Paradisi ¹, Cristina Siligardi ^{1,2}
and Isabella Lancellotti ^{1,2,*}

¹ Department of Engineering “Enzo Ferrari”, University of Modena and Reggio Emilia, 41125 Modena, Italy; caterina.sgarlata@unimore.it (C.S.); mariacamila.arizatarazona@unimore.it (M.C.A.-T.); enrico.paradisi@unimore.it (E.P.); cristina.siligardi@unimore.it (C.S.)

² National Interuniversity Consortium of Materials Science and Technology (INSTM), 50121 Florence, Italy

* Correspondence: isabella.lancellotti@unimore.it

Abstract: The aim of this research was to evaluate the possibility of reusing waste foundry sands derived from the production of cast iron as a secondary raw material for the production of building materials obtained both by high-temperature (ceramic tiles and bricks) and room-temperature (binders such as geopolymers) consolidation. This approach can reduce the current demand for quarry sand and/or aluminosilicate precursors from the construction materials industries. Samples for porcelain stoneware and bricks were produced, replacing the standard sand contained in the mixtures with waste foundry sand in percentages of 10%, 50%, and 100% by weight. For geopolymers, the sand was used as a substitution for metakaolin (30, 50, 70 wt%) as an aluminosilicate precursor rather than as an aggregate to obtain geopolymer pastes. Ceramic samples obtained using waste foundry sand were characterized by tests for linear shrinkage, water absorption, and colorimetry. Geopolymers formulations, produced with a Si/Al ratio of 1.8 and Na/Al = 1, were characterized to evaluate their chemical stability through measurements of pH and ionic conductivity, integrity in water, compressive strength, and microstructural analysis. The results show that the addition of foundry sand up to 50% did not significantly affect the chemical-physical properties of the ceramic materials. However, for geopolymers, acceptable levels of chemical stability and mechanical strength were only achieved when using samples made with 30% foundry sand as a replacement for metakaolin.

Keywords: foundry sands; waste; ceramic products; bricks; geopolymers



Citation: Sgarlata, C.;

Ariza-Tarazona, M.C.; Paradisi, E.;

Siligardi, C.; Lancellotti, I. Use of

Foundry Sands in the Production of

Ceramic and Geopolymers for

Sustainable Construction Materials.

Appl. Sci. **2023**, *13*, 5166. [https://](https://doi.org/10.3390/app13085166)

doi.org/10.3390/app13085166

Academic Editor: José Manuel

Moreno-Maroto

Received: 22 March 2023

Revised: 13 April 2023

Accepted: 19 April 2023

Published: 21 April 2023



Copyright: © 2023 by the authors.

Licensee MDPI, Basel, Switzerland.

This article is an open access article

distributed under the terms and

conditions of the Creative Commons

Attribution (CC BY) license ([https://](https://creativecommons.org/licenses/by/4.0/)

[creativecommons.org/licenses/by/](https://creativecommons.org/licenses/by/4.0/)

[4.0/](https://creativecommons.org/licenses/by/4.0/)).

1. Introduction

Foundry sands consist primarily of clean, uniformly sized, high-quality silica sand used in the production of molds for both ferrous (iron and steel) and nonferrous (copper, aluminum, and brass) metal casting industries.

Molding sands are obtained by adding binding agents to virgin silica sands. Silica sand is mainly used because of its thermal conductivity. It can absorb and transmit heat while allowing the gases generated during the thermal degradation of binders to pass through the grains. In general, molding sand is extensively used because it is easy to use, economical, has high-temperature resistance, and due to its ability to bind with other binders and organic materials, outperforming natural sand [1].

According to their composition, foundry sands are classified into two types: green sands and chemical foundry sands. Green sands are composed of 85–95% silica sand, 4–10% bentonite clay as a binder, 2–10% of carbonaceous additive, and water (2–5%); they are particularly suitable for geotechnical applications, such as structural fills and base courses. Chemical foundry sands are composed of 93–99% silica sand and 1–3% chemical binder; they are used as the “cores” in castings to withstand the heat of molten metal and as molds for nonferrous castings [2].

In the casting process, molding sands are recycled and reused multiple times, but after going through many production cycles, they become less uniform and lose their cleanliness. The sand grains begin to break down because of heat and mechanical abrasion, and therefore new sand must be continually added to the system. When waste foundry sands (WFS) are no longer suitable for the manufacturing process, they are removed from the system and discarded at foundry landfills or offsite municipal landfills [2].

It is estimated that approximately 100 million tons of sand are used in annual production, and 6–10 million tons are discarded annually and available to be recycled into other products and industries [3]. Further, about one ton of foundry sand is used for each ton of iron or steel casting produced [4]. Meanwhile, the foundry industry in Italy produces 1.5 million tons of raw casting and generates about one million tons of waste, most of which (around 80%) is sand. The automotive industries are the major generators of foundry sand (about 95% of the estimated WFS) [2].

As millions of tons of waste foundry sands are generated each year, their disposal has become an environmental challenge [5]. Foundry sand can be classified as a hazardous or non-hazardous material, depending on its source. Silica-based spent foundry sands, specifically from iron, steel, and aluminum foundries, are considered non-hazardous, while spent foundry sands from leaded brass and bronze foundries are often regulated as hazardous waste because of the presence of highly toxic organic pollutants that can contaminate the atmosphere or condense in the sand. These pollutants include phenols and inorganic elements such as lead, chromium, cadmium, iron, and zinc [6]. Even though the analysis of the leachate obtained from waste foundry sands has found that the concentration of most hazardous substances is below the acceptable limits, hazardous polyaromatic hydrocarbons have been found in all types of waste foundry sands [6]. Waste foundry sands should be dumped into controlled landfills; however, because of the growing waste foundry sands production and the need for landfill monitoring, the landfilling cost has been continuously increasing in the past years, reaching \$135–657 million in the U.S.A. [7], making unviable to continue with this practice.

Consequently, recycling waste foundry sands into several applications has become an attractive opportunity to decrease the economic and environmental impact of their disposal [8]. Although natural materials are often preferred in terms of quality, their sources are depleting gradually over the years, making the use of waste materials viable [7,9,10].

Silica-based WFSs are classified as non-hazardous residues and can be used in other industries as secondary raw materials. For example, they have been used in the sustainable building sector, specifically in cold consolidated materials such as cementitious conglomerates, asphalts, concrete, and cement [11]. Ceramic materials regulations allow the use of secondary residual raw materials to replace sands normally used as inert material in the production of ceramic tiles and bricks, therefore contributing to the reduction of the environmental impact of their activities [12]. Other types of products suitable for exploiting foundry sands are geopolymers, materials obtained through the cold alkaline activation of suitable precursors. In geopolymers, foundry sands are potentially interesting as precursors and/or as fillers or aggregates to obtain geopolymer mortars [12,13]. In this work, we investigated the potential application of WFS, obtained from different Italian metal casting industries, in geopolymers and ceramic tiles formulations.

2. Materials and Methods

2.1. Waste Foundry Sands

The waste foundry sand (WFS) used for ceramic tile (porcelain stoneware) and bricks application is named 31A. For the geopolymers application, foundry sand with higher content of aluminum was chosen and is named 17A. The chemical composition of the sands was analyzed through an XRF spectrometer (Bruker S4 Pioneer), and it is reported in Table 1. As expected, SiO₂ is present in high quantities in both samples, but 31A has a higher amount of it compared to 17A. Furthermore, 31A has small amounts of Al, Fe, and Zr. In comparison, 17A sand has a higher amount of aluminum, which is useful for

alkali activation, Fe, and Zr, and presents an organic fraction that is evident from both carbon content (4.350%) and LOI (6.2%). Given that the geopolymers were obtained at room temperature, the organic content does not represent a problem with respect to samples that need firing. Traces of sulfur are also present.

Table 1. Chemical composition of sands 17A and 31A.

XRF	SiO ₂	Al ₂ O ₃	TiO ₂	Fe ₂ O ₃	CaO	MgO	K ₂ O	Zr ₂ O	L.O.I.	C	S
	(%)	(%)	(%)	(%)	(%)	(%)	(%)	(%)	(%)	(%)	(%)
17A	81.85	2.83	0.15	3.88	0.13	0.48	0.32	4.15	6.20	4.350	0.385
31A	93.00	2.03	0.37	1.48	0.12	0.16	0.71	1.89	0.24	0.177	0.046

2.2. Particle Size Distribution Analysis

The size and distribution of particles were determined using a Mastersizer 2000 Light Diffractometer. The sands were initially sieved using a 1 mm sieve and then were measured using the light diffractometer.

2.3. X-ray Diffraction (XRD)

X-ray diffractions were recorded by a PW3710 diffractometer (Philips, Almelo, The Netherlands). Specimens were scanned in the 0–70° 2θ angular range on powdered samples, using Cu-Kα radiation from a conventional X-ray source operated at 35 kV, 35 mA, and a scan step of 0.02°. The patterns were analyzed using the HighScore Plus (PANalytical) software.

2.4. Samples Formulation and Preparation

The materials used for ceramic tiles are clays and feldspars of different origins and standard sand. The standard sand was replaced in varied percentages with the foundry sand, as reported in Table 2. For brick materials, different types of clays and basalt were used. The basalt, as for the sand in ceramics tiles, was replaced with the foundry sand, as reported in Table 3.

Table 2. Formulations of porcelain stoneware samples.

Composition (%) Material	STD	SF10	SF50	SF100
Clay 1	26	26	26	26
Clay 2	14	14	14	14
Feldspar 1	20	20	20	20
Feldspar 2	28	28	28	28
Sand	12	10.8	6	0
Foundry sand	0	1.2	6	12

Table 3. Formulations of brick samples.

Composition (%) Material	FSTD	F.10	F.50	F.100
Clay (Vicenza)	33.30	33.30	33.30	33.30
Marl (Possagno)	23.40	23.40	23.40	23.40
Clay Modena 1	16.65	16.65	16.65	16.65
Clay Modena 2	16.65	16.65	16.65	16.65
Basalt fine	10.00	9.00	5.00	0
Foundry sand	0	1.00	5.00	10.00

For tile samples, the standard mixture shown in Table 2 was used. Raw materials were mixed with water in a 2:1 ratio, and a fluidizer was added to improve the pourability of the dough. Then the dried dough was pulverized and humidified to 6% before being pressed to obtain the samples and cooked up to 1205 °C.

For brick mixtures, the raw materials previously dried and sieved under 500 µm were mixed with around 27% water to obtain a smooth and malleable dough suitable for extrusion. Then, samples were extruded and cut to a size of 5 × 2 cm and dried at room temperature and then at 105 °C. Subsequently, the samples were put in the stove up to 1050 °C.

For the geopolymers application, the foundry sand 17A corresponding to a higher ratio of aluminum to silicon, was chosen. As a matrix for geopolymer samples, metakaolin CSC1000-ARGICAL 1000 provided by Bal-Co (Sassuolo, MO, IT) was used. As activating solutions, sodium silicate provided by Ingessil (Montorio, Vr, IT) and NaOH 8 M provided by Merck-Sigma-Aldrich (Milano, IT) were used.

The fresh pastes were prepared by mixing metakaolin and waste sand with the activating solution (NaOH and Na₂SiO₃) into a container with a mechanical mixer for approx. 10 min. When the geopolymer paste was homogenous and achieved suitable workability, it was poured into a mold and covered with a plastic film. The samples were cured at room temperature for 28 days before further characterization.

A standard mixture of geopolymer was initially prepared using 100% metakaolin and reacted with 30 mL of NaOH 8M and 30 mL of sodium silicate. In the other formulations, part of metakaolin (30%, 50%, and 70% by weight) was replaced with waste sand 17A, and the collected results of chemical stability, durability in water, and mechanical resistance were compared.

2.5. Ceramic Samples Characterization

2.5.1. Linear Shrinkage

Linear shrinkage has been calculated for samples according to the following expression:

$$LS\% = \frac{d_i - d_f}{d_i} \times 100$$

where:

- d_i = initial diameter (40 mm),
- d_f = final diameter.

The results are given as the mean of the 3 measurements taken for the same specimen.

2.5.2. Water Absorption

For water absorption tests, samples with known weight were immersed in boiling water for two hours. Then they were extracted, dried on the surface, and weighed again. The water absorption was obtained as follows:

$$WA\% = \frac{W_B - W_S}{W_S} \times 100$$

where:

- W_B = wet sample weight
- W_S = dry sample weight.

2.5.3. Colorimetry

The measures were performed using a PCE-CSM 6 instrument that operates in the CIE L*a*b* color space. The color space model allows for the accurate representation of colors using three coordinates. The L*a*b* mode covers the entire visible spectrum of the human eye and allows you to describe the set of colors perceived by sight.

This analysis was carried out on a sample of each formulation: for each of them, 5 measurements were taken at different points on the surface in order to evaluate possible color variations, which are described by ΔE , defined as:

$$\Delta E = \sqrt{(L_2 - L_1)^2 + (a_2 - a_1)^2 + (b_2 - b_1)^2}$$

By convention, two colors appear indistinguishable when $\Delta E < 1$. In practice, a $\Delta E = 1$ is considered a good commercial result.

2.6. Geopolymeric Samples Characterization

2.6.1. Integrity Test

The integrity test is a preliminary qualitative test used to assess the material and its stability in an aqueous environment in order to verify if the geopolymerization process has occurred. The integrity test is carried out at room temperature (20 ± 5 °C) using a solid/liquid ratio of 1:100 in static conditions and for a duration of 24 h. During the test, a portion of the sample is immersed into a beaker with distilled water, and after 24 h, the integrity of the portion of the sample within the beaker is visually evaluated. The occurrence of the geopolymerization reaction is confirmed if the sample does not dissolve in water [14].

2.6.2. pH and Ionic Conductivity Measures

Measures of pH and ionic conductivity were performed by immersing a portion of the sample under stirring conditions at 20 ± 2 °C in deionized water with a solid/liquid ratio of 1/10 for 24 h. Ionic conductivity and pH of the eluate solutions were determined at different times (0, 5, 15, 30, 60, 120, 240, 360, 1440 min) to obtain a trend of the change in value during the 24 h and to have information on the amount of dissolved solid [15]. The pH was detected with a Hamilton-type Liq-glass SL Laboratory pH sensor (Hamilton A.G., Bonaduz, Switzerland), and the ionic conductivity of the solution was measured with a calibrated cell, both of which were connected to the digital display of pH 5/6 and Ion 6-Oakton/Eutech Instruments (Oakton Instruments, Vernon Hills, IL, USA).

2.6.3. Mechanical Resistance

Mechanical resistance of samples was measured through the compressive strength of cubic samples ($20 \times 20 \times 20$ mm³) using an Instron 5567 Universal Testing Machine with a 30 kN load limit and 1 mm/min of displacement, according to the standard UNI EN 826, after 28 days of curing. Compressive strength values are given as the mean value of four tests accompanied by a 2% variance.

3. Results and Discussion

3.1. Waste Foundry Sands Characterization

The diffractograms for 31A and 17A sands are reported in Figure 1. The 31A sand presents peaks corresponding to quartz SiO₂ (Q), microcline K-feldspar KAlSi₃O₈ (K), and zircon ZrSiO₄ (Z). The diffractogram of 17A presents peaks corresponding to quartz SiO₂ (Q), calcite CaCO₃ (C), hematite Fe₂O₃ (H), and mullite Al₆Si₂O₁₃ (M). The main phase consists of quartz, SiO₂ (Q), for both sands.

3.2. Particle Size Distribution

Figure 2a shows the particle size distribution for 31A sand. From the graph, it can be inferred that the particle size of this sample is homogeneous and is around 100 μm. Figure 2b shows the particle size distribution of 17A sand, which is courser with respect to 31A sand and centered around 500–600 μm with a small number of particles showing a size lower than 100 μm. For geopolymer formulations, sand 17A was ground to have a particle size ≤ 125 μm in order to favor the reactivity in an alkaline environment.

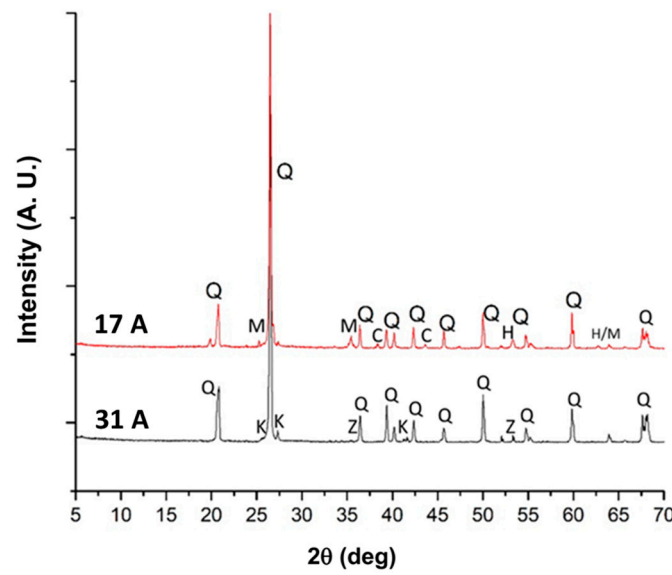
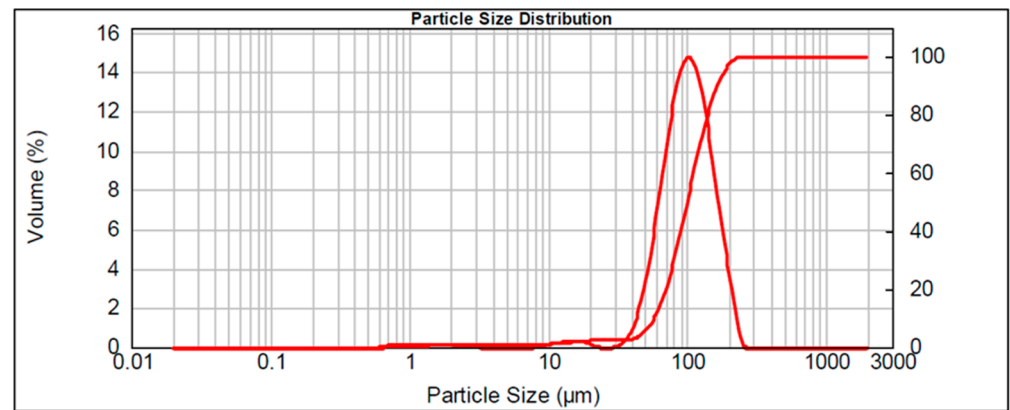
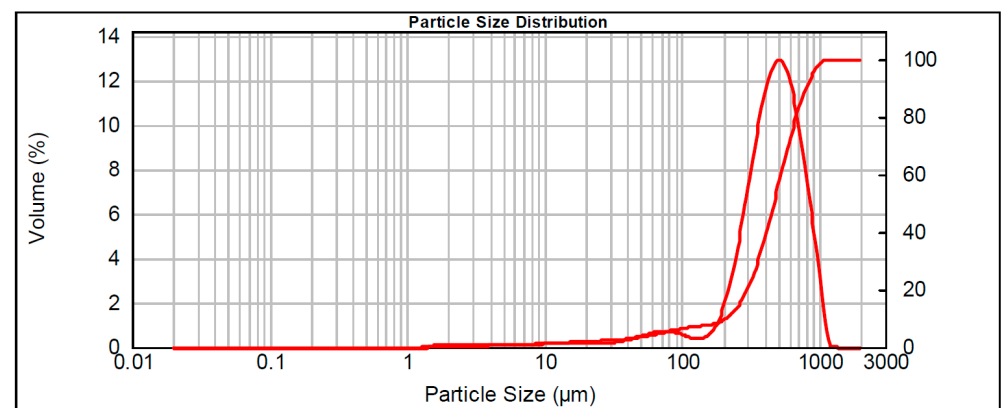


Figure 1. X-ray diffraction of 31A and 17A sands (Q = Quartz, K = Microcline K-feldspar, Z = Zircon, M = Mullite, H = Hematite, C = Calcite).



(a) 31A



(b) 17A

Figure 2. Particle size distribution of 31A (a) and 17A (b) sands.

3.3. Porcelain Stoneware

The results of linear shrinkage, water absorption, and colorimetry of porcelain stoneware samples produced using 10%, 50%, and 100% of waste sand, are reported in Table 4 and compared to the standard formulation (STD). The values show a linear shrinkage of around 4.8% for almost all the formulations. There is a slight decrease of this value, corresponding

to slightly less sintering, when the replacement of STD sand with foundry sand is higher than 50%, but spent foundry sand does not significantly affect linear shrinkage.

Table 4. Results of linear shrinkage (LS%), water absorption (AA%), and colorimetry (ΔE) with standard deviation (St.Dev) of porcelain stoneware samples.

Porcelain Stoneware	LS%	St.Dev	WA%	St.Dev	ΔE
STD	4.8	0.3	0.009	0.004	0
SF10	4.7	0.1	0.0015	0.0002	0
SF50	4.9	0.2	0.022	0.003	1
SF100	4.3	0.1	0.02	0.01	1.73

For water absorption tests, it can be observed that the absorption obtained for each formulation is lower than 0.025% WA, despite a slight increase observed with the addition of sand in quantities exceeding 50%. From these results, it can be deduced that, despite the addition of foundry sand, the obtained stoneware remains a low porosity material, according to the norm UNI EN 176 ISO BI.

For colorimetry measures, the values of ΔE in relation to the reference sample STD show that the addition of foundry sand to the mixture does not lead to significant color variations. In fact, all the samples have almost the same color. The biggest difference is observed between the STD sample and the SF100% sample where $\Delta E = 1.73$, so the color variation begins to be distinguishable, but the overall difference could be accepted.

The diffractograms obtained from the XRD analysis of SF100 and STD are both shown in Figure 3 for comparison. The main difference between them is the presence of the Microcline intermediate phase in sample SF100 (highlighted in the inset graph), which is not observed in the STD sample. It is also possible to observe a different intensity of the peaks at $28^\circ 2\theta$ corresponding to albite, higher for sample SF100 compared with the STD. Anyway, these differences can be considered relatively small, as both diffractograms show mainly the same crystalline phases (quartz, mullite, and albite).

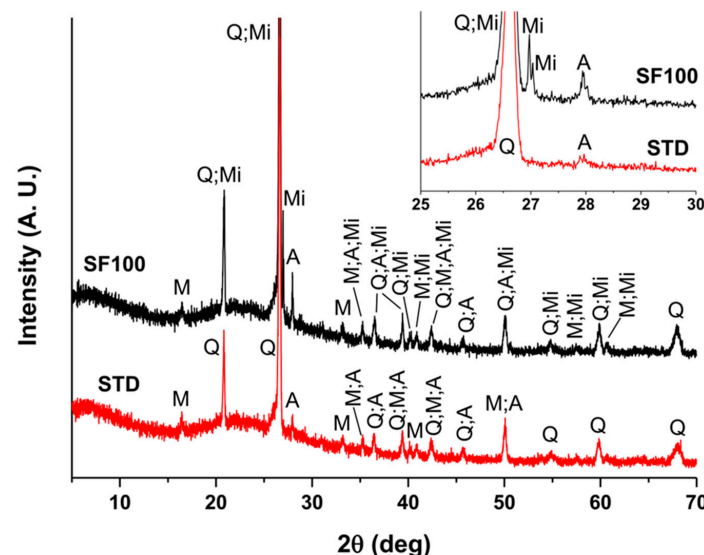


Figure 3. X-ray diffraction of samples SF100 and STD (Q = Quartz, Mi = Microcline intermediate, M = Mullite, A = Albite).

3.4. Bricks

The results of linear shrinkage, water absorption, and colorimetry of brick samples produced using 10%, 50%, and 100% of waste sand are reported in Table 5 and compared to the standard formulation STD. The post-firing linear shrinkage (LS%) shows a slight

increase by adding the foundry sand. The presence of Fe in the foundry sand can influence this behavior.

Table 5. Results of linear shrinkage (LS%), water absorption (AA%), and colorimetry (ΔE) with standard deviation (St.Dev) of brick samples.

Brick Sample	LS%	St.Dev	WA%	St.Dev	ΔE
F.STD	5.2	0.9	8.6	0.4	0
F.10	6.6	0.8	10.8	0.41	1.49
F.50	6	1	12.1	0.5	1.15
F.100	6	1	12.7	0.7	2.84

The water absorption values for brick samples increase with the amount of foundry sand added. The higher value of WA% was shown by sample F.100 with 12.7 WA%, compared to 8.65 WA% shown by the standard formulation with basalt. This means that, despite the addition of foundry sand, brick samples remain a highly porous material [16].

For colorimetry measures, the ΔE values of samples depend on the amount of sand added. The ΔE measures are in the range of 2–3 for all samples compared to the standard formulation, so it can be deduced that there is a distinguishable color variation.

In Figure 4, the diffractograms obtained for the brick formulations are reported. Even in this case, there are no particular differences between the diffractograms of F.100 and F.STD samples, which show peaks of the same crystalline phases (quartz, hematite, and albite), with a negligible variation in their intensity, due to the variation in the percentage of foundry sand added.

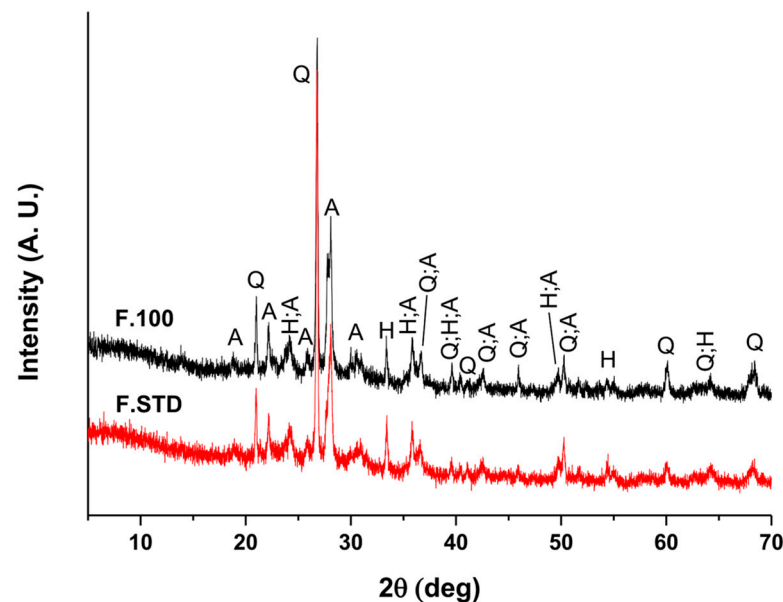


Figure 4. X-ray diffraction of F.100 and F.STD (Q = Quartz, H = Hematite, A = Albite).

From the analyses carried out, it is possible to conclude that the introduction of foundry sand as a secondary raw material for tiles and bricks in place of virgin sand modifies the physical properties of the standard samples in an acceptable way. The results obtained using waste foundry sands for ceramic materials may be considered acceptable, compared to similar studies with waste materials found in the literature for tiles and porcelain stoneware, e.g., in terms of water absorption and shrinkage [17,18] and for bricks [19], on the application which they are intended.

3.5. Geopolymer

The geopolymer formulations are reported in Table 6, with the respective Si/Al molar ratio, which increases by increasing the foundry sand content because the waste is poor in aluminum with respect to metakaolin.

Table 6. Sample compositions of geopolymer formulation.

Name	MK (g)	WFS (g)	NaOH 8M (mL)	Na ₂ SiO ₃ (mL)	Si/Al
100% MK	100	0	30	30	1.4
70% MK	70	30	30	30	1.82
50% MK	50	50	30	30	2.27
30% MK	30	70	30	30	3

The integrity test of samples containing 30%, 50%, and 70% of foundry sand showed that the color of the immersion water became darker by increasing the amount of sand in the formulation, but it remained transparent. The change in color of the immersed water may be an indication of the release of elements from the sample into the water and their subsequent decrease in chemical stability.

When samples lose their structural consistency, and the water of immersion becomes cloudy, the formulation is not considered acceptable. This is a qualitative indication of the stability of formulations that will then be quantified by pH and ionic conductivity tests to indirectly evaluate the efficacy of reticulation reactions. Even when the alkaline solution does not react completely with aluminosilicate powders, it may have still leached out during immersion of the sample in water. In this case, almost all samples remain intact after 24 h, so the integrity test is considered passed.

In Figure 5 (left), the pH measurements of 30% MK, 50% MK, and 70% MK samples after 24 h are compared with 100% MK. It was noted that the pH value increased over time at short immersion times while remaining constant or even decreasing at longer immersion times. The pH of the eluate after 24 h is in a range between 10 and 11 for all samples, confirming the typical alkalinity of these samples. The standard 100% MK shows pH values between 11.19 at 30 min and 10.73 at 1440 min (24 h) [20].

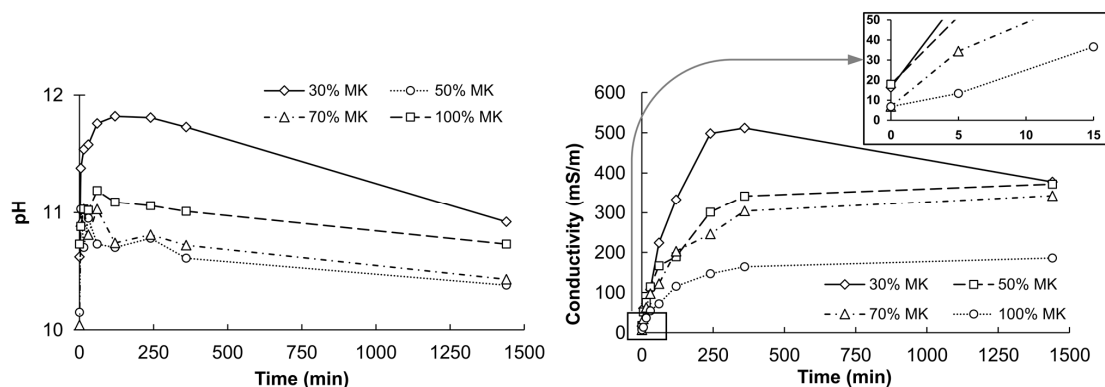


Figure 5. Results of pH (left) and ionic conductivity (right) of geopolymer samples cured at room temperature. Zoom of ionic conductivity: sharp rise of conductivity during the first minutes.

Figure 5 (right) shows the conductivity measurements carried out on the same samples. The highest ionic conductivity is recorded by the sample with the lowest amount of metakaolin (30% MK), which after 8 h reaches a value of about 500 mS/m but then stabilizes within 24 h at 378 mS/m, similar to the value of 50% MK sample with 372 mS/m. The sample having the highest amount of metakaolin (70% MK) exhibited an overall lower value, approaching the standard 100% MK, with a conductivity of 300 mS/m after 8 h of testing.

This behavior follows the typical trend of alkali-activated materials found in literature, and it is related to the lower stability of samples with a very high addition of sand [21].

Figure 6 shows the results of the compression strength tests on samples after the curing time of 28 days. There is a strong dependence of the values on the percentage of MK present in the formulations. In fact, the compressive strength decreases by decreasing the amount of MK. In Figure 6, the values of the Si/Al ratio for each sample are shown as orange points. Mechanical properties improve as the Si/Al ratio decreases to around 1.4–1.8. Acceptable results were, however, achieved for sample 70% MK showing a value around 21 MPa, compared to the standard 100% MK [22], so the addition of a 30% foundry sand is considered feasible.

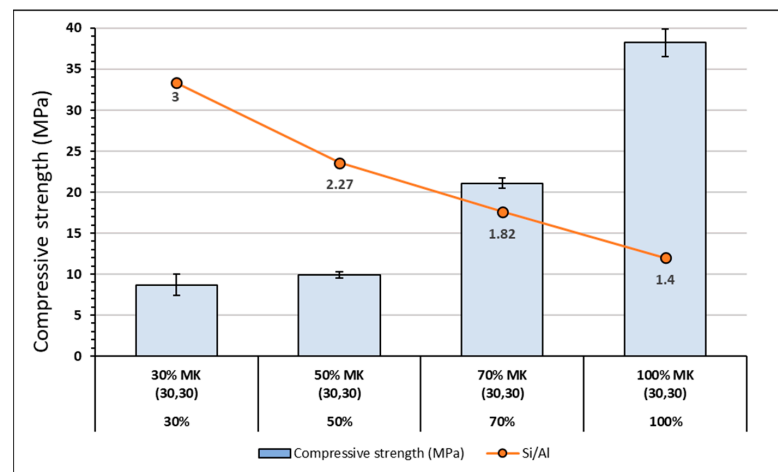


Figure 6. Results of compressive strength for geopolymer samples.

XRD patterns of 70% MK sample and 17A foundry sand are shown in Figure 7. In the sample with 70% MK, the presence of the broadband between 15–35° 2 θ can be observed, which is characteristic of the amorphous phase that for pure metakaolin-based geopolymers is positioned between 25–32° 2 θ [23]. The presence of this broadband (blue circled in Figure 7) confirms that the presence of foundry sand does not hinder the geopolymerization process, but some degree of crystallinity is maintained due to the nature of sand: this behavior is already observed in literature for geopolymers where wastes with a complex semicrystalline nature were used in place of metakaolin [24].

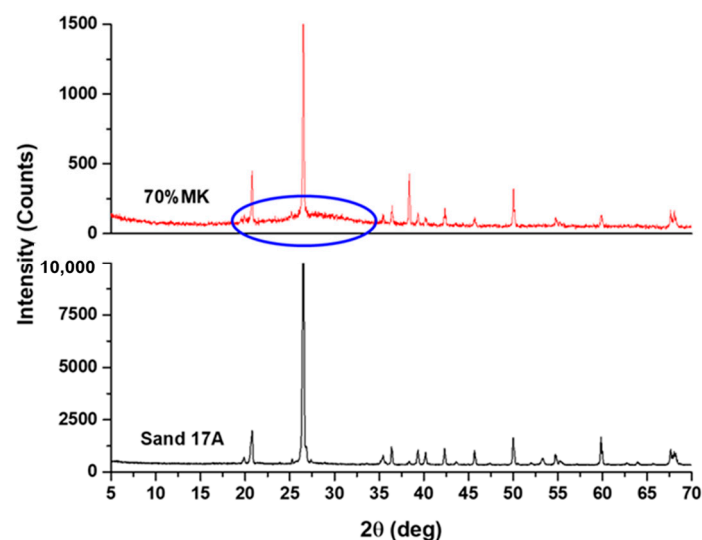


Figure 7. XRD patterns of 70% MK sample and 17A foundry sand.

4. Conclusions

In this work, the potential application of WFSs obtained from different Italian metal casting industries in geopolymers and ceramic materials was investigated.

For porcelain stoneware, the value of linear shrinkage was found to be in the range of 4.3–4.8% for all the formulations (10%, 50%, and 100%), and the values of water absorption (<0.02%) indicate that the obtained material, despite the addition of foundry sand, remains a low porosity material. The XRD diffractograms confirm that there are no relevant differences between them.

Colorimetry measures revealed that the biggest difference is observed between the STD sample and the SF100% sample with $\Delta E = 1.73$.

For bricks, the addition of foundry sand only slightly affects the post-firing linear shrinkage, showing an increase of the same, as well as for the water absorption. Even with the addition of foundry sand, brick samples remain a highly porous material, and no differences in the crystalline phases present are detected. Even the ΔE values of samples depend on the amount of sand added, with a distinguishable color variation.

For geopolymer formulations, the results of chemical stability, pH and ionic conductivity, and compression strength tests show that there is a strong dependence of the values on the percentage of MK present in the formulations, and the properties of samples worsen with the decrease of MK.

In summary, foundry sand can be used in partial or total substitution to the sand that is typically used as standard, at least when the colorimetric aspect is not of primary importance. So, it can potentially be used for formulations that are not associated with large tile formats where aesthetic needs are relevant.

It is thus possible to obtain acceptable results on the properties of the final materials by replacing virgin sand with foundry sand in geopolymer formulations (although in percentages not exceeding 30%). Further studies could be carried out to optimize the obtained results, thus improving the performance of geopolymer samples containing foundry sand.

Author Contributions: Conceptualization, C.S. (Cristina Siligardi) and I.L.; methodology, C.S. (Cristina Siligardi); investigation, E.P. and M.C.A.-T.; data curation, M.C.A.-T.; writing—original draft preparation, C.S. (Caterina Sgarlata); writing—review and editing, C.S. (Caterina Sgarlata) and I.L.; supervision, I.L. and C.S. (Cristina Siligardi); project administration, I.L.; funding acquisition, I.L. All authors have read and agreed to the published version of the manuscript.

Funding: This research was funded by INSTM and Fondazione Cariplo-2020_1216, project title: New recycling process for the foundry sands for Action D- Evaluation and assessment of novel routes for waste sands recovery.

Institutional Review Board Statement: Not applicable.

Informed Consent Statement: Not applicable.

Data Availability Statement: Not applicable.

Acknowledgments: The authors recognize Utilizzo Di Sabbie Di Fonderia Nella Produzione Di Ceramiche E Geopolimeri Per L'edilizia Sostenibile within Project Cariplo-2020_1216 for Action D- Evaluation and the assessment of novel routes for waste sands recovery.

Conflicts of Interest: The authors declare no conflict of interest.

References

1. Ahmad, J.; Zhou, Z.; Martínez-García, R.; Vatin, N.L.; De-Prado-Gil, J.; El-Shorbagy, M.A. Waste Foundry Sand in Concrete Production Instead of Natural River Sand: A Review. *Materials* **2022**, *15*, 2365. [[CrossRef](#)] [[PubMed](#)]
2. Tittarelli, F. Waste foundry sand. In *Waste and Supplementary Cementitious Materials in Concrete*; Elsevier: Amsterdam, The Netherlands, 2018; pp. 121–147.
3. Babu, G.M.; Dadapeer, A.B.S. An Experimental Investigation on Effects of Foundry sand on Concrete Interms of Characteristics of Strength. *J. Emerg. Technol. Innov. Res.* **2018**, *5*, 154–161.

4. Siddique, R.; Noumowe, A. Utilization of spent foundry sand in controlled low-strength materials and concrete. *Resour. Conserv. Recycl.* **2008**, *53*, 27–35. [[CrossRef](#)]
5. Son, B.T.; Long, N.V.; Hang, N.T.N. Fly ash-, foundry sand-, clay-, and pumice-based metal oxide nanocomposites as green photocatalysts. *RSC Adv.* **2021**, *11*, 30805–30826. [[CrossRef](#)]
6. Iqbal, M.F.; Liu, Q.-F.; Azim, I.; Zhu, X.; Yang, J.; Javed, M.F.; Rauf, M. Prediction of mechanical properties of green concrete incorporating waste foundry sand based on gene expression programming. *J. Hazard. Mater.* **2020**, *384*, 121322. [[CrossRef](#)]
7. Siddique, R.; Singh, G.; Singh, M. Recycle option for metallurgical by-product (Spent Foundry Sand) in green concrete for sustainable construction. *J. Clean. Prod.* **2018**, *172*, 1111–1120. [[CrossRef](#)]
8. Gambalonga, B.; Nicolini, J.L.; Inocente, J.M.; Pich, C.T.; Angioletto, E.; Pereira, F.R.; Montedo, O.P.K.; Arcaro, S. Valorization of waste foundry sand aggregates in hot-mix asphalt. *Process Saf. Environ. Prot.* **2023**, *173*, 277–288. [[CrossRef](#)]
9. Abdulhameed, H.; Mansi, A.; Mohammed, A.; Abdulhameed, A.; Hanoon, A. Study the use of Nano-limestone and Egg-shell Ash in Eco-friendly SCC: An Experimental and Statistical Evaluation Based on Computer Programming. In Proceedings of the 14th International Conference on Developments in eSystems Engineering (DeSE), Sharjah, United Arab Emirates, 7–10 December 2021; pp. 509–514. [[CrossRef](#)]
10. Murmu, A.L.; Patel, A. Towards sustainable bricks production: An overview. *Constr. Build. Mater.* **2018**, *165*, 112–125. [[CrossRef](#)]
11. Luqman, A.L.I.; Khan, M.N.A.; Rasheed, Y. Effect of Waste Foundry Sand (WFS) on Strength and Durability of Pressed Fired Clay Bricks. In Proceedings of the ND Conference on Sustainability in Civil Engineering (CSCE'20), Department of Civil Engineering, Capital University of Science and Technology, Islamabad, Pakistan, 12 August 2022.
12. Dyer, P.P.O.L.; Klinsky, L.M.G.; Silva, S.A.; Silva, R.A.; Lima, M.G. Macro and microstructural characterization of waste foundry sand reused as aggregate Road. *Mater. Pavement Des.* **2021**, *22*, 464–477. [[CrossRef](#)]
13. Patil, A.R.; Sathe, S.B. Feasibility of sustainable construction materials for concrete paving blocks: A review on waste foundry sand and other materials. *Mater. Today Proc.* **2020**, *43*, 1552–1561. [[CrossRef](#)]
14. Piccolo, F.; Andreola, F.; Barbieri, L.; Lancellotti, I. Synthesis and Characterization of Biochar-Based Geopolymer Materials. *Appl. Sci.* **2021**, *11*, 10945. [[CrossRef](#)]
15. Lancellotti, I.; Ponzoni, C.; Barbieri, L.; Leonelli, C. Alkali activation processes for incinerator residues management. *Waste Manag.* **2013**, *33*, 1740–1749. [[CrossRef](#)] [[PubMed](#)]
16. Hossiney, N.; Das, P.; Mohan, M.K.; George, J. In-plant production of bricks containing waste foundry sand—A study with Belgaum foundry industry. *Case Stud. Constr. Mater.* **2018**, *9*, e00170. [[CrossRef](#)]
17. Yuan, Q.; Robert, D.; Mohajerani, A.; Tran, P.; Pramanik, B.K. Utilisation of waste-to-energy fly ash in ceramic tiles. *Constr. Build. Mater.* **2022**, *347*, 128475. [[CrossRef](#)]
18. Dondi, M.; Raimondo, M.; Zanelli, C. Clays and bodies for ceramic tiles: Reappraisal and technological classification. *Appl. Clay Sci.* **2014**, *96*, 91–109. [[CrossRef](#)]
19. Arias-Trujillo, J.; Matías-Sánchez, A.; Cantero, B.; López-Querol, S. Effect of polymer emulsion on the bearing capacity of aeolian sand under extreme confinement conditions. *Constr. Build. Mater.* **2019**, *236*, 117473. [[CrossRef](#)]
20. Sun, Z.; Vollpracht, A.; van der Sloot, H.A. pH dependent leaching characterization of major and trace elements from fly ash and metakaolin geopolymers. *Cem. Concr. Res.* **2019**, *125*, 105889. [[CrossRef](#)]
21. Galiano, Y.L.; Pereira, C.F.; Vale, J. Stabilization/solidification of a municipal solid waste incineration residue using fly ash-based geopolymers. *J. Hazard. Mater.* **2011**, *185*, 373–381. [[CrossRef](#)]
22. Rajamma, R.; Labrincha, J.A.; Ferreira, V.M. Alkali activation of biomass fly ash–metakaolin blends. *Fuel* **2012**, *98*, 265–271. [[CrossRef](#)]
23. Pinheiro, D.D.R.; Gonçalves, L.R.; Sena, R.L.P.D.; Martelli, M.C.; Neves, R.D.F.; Ribeiro, N.F.D.P. Industrial Kaolin Waste as Raw Material in the Synthesis of the SAPO-34 Molecular Sieve. *Mater. Res.* **2020**, *23*. [[CrossRef](#)]
24. Sarkar, M.; Dana, K. Partial replacement of metakaolin with red ceramic waste in geopolymer. *Ceram. Int.* **2020**, *47*, 3473–3483. [[CrossRef](#)]

Disclaimer/Publisher's Note: The statements, opinions and data contained in all publications are solely those of the individual author(s) and contributor(s) and not of MDPI and/or the editor(s). MDPI and/or the editor(s) disclaim responsibility for any injury to people or property resulting from any ideas, methods, instructions or products referred to in the content.